Author(s): Melander, Marko M.

Title: Frozen or dynamic? : An atomistic simulation perspective on the timescales of electrochemical reactions

Year: 2023

Version: Published version

Please cite the original version:

Melander, M. M. (2023). Frozen or dynamic? : An atomistic simulation perspective on the timescales of electrochemical reactions. Electrochimica Acta, 446, Article 142095. https://doi.org/10.1016/j.electacta.2023.142095

Electrochimica Acta 446 (2023) 142095

Contents lists available at ScienceDirect

Electrochimica Acta

journal homepage: www.journals.elsevier.com/electrochimica-acta

Frozen or dynamic? — An atomistic simulation perspective on the timescales of electrochemical reactions

Marko M. Melander

Department of Chemistry and Nanoscience Center, University of Jyväskylä, Finland, P.O. Box 35, (YN), Jyväskylä, FI-40014, Finland

ARTICLE INFO

MSC:
0000
1111

Keywords:
Electrocatalysis
Solvent reorganization
Sampling
Proton-coupled electron transfer
Electrolyte

ABSTRACT

Electrochemical systems span a wide range of timescales, and several recent works have put forth the idea that the reaction environment should remain frozen and out of equilibrium during electrochemical electron or proton transfer reactions. Furthermore, simplified treatments of the electrochemical interface model the solvent and ions as frozen molecules. However, the claims and practices of a frozen environment strongly clash with most theoretical and simulation approaches developed to study electrochemical reaction rates. It has also been suggested that the electrode potential should not be fixed when simulating reaction rates due to conductivity limitations, which indicates constant potential simulations to be incorrect. In this critical review, these claims re-analyzed from the perspective of non-ergodic rate theory, which provides a rigorous framework to determine when or whether the reaction environment should appear frozen: it is shown that in most activated electrochemical reactions in aqueous media, the reaction environment is completely mobile and equilibrated under constant potential conditions. Only for ultrafast reactions or transient methods should the environment be considered (partly) frozen and in a non-equilibrium state. For both metallic and practical semiconductor electrodes the impact of electrode conductivity is minimal and constant potential calculations are found reliable. The implications of these considerations are be discussed from a viewpoint of computational and theoretical electrochemistry.

1. Introduction

Electrochemical interfaces (ECIs) are extremely complicated reaction environments. Besides various competing interactions, [1] processes at ECIs span several relevant timescales from sub-femtosecond electron dynamics to diffusion and electrode disintegration taking place on the microsecond or even year timescales, respectively. Simulating the different time and lengthscales involved in these processes calls for high-level multiscale methods.

Here I focus on timescales relevant to elementary reaction kinetics in the sub-microsecond range. The goal of this perspective is to analyze in detail which timescales and processes should be included in fully atomistic simulations of electrochemical interfaces. The analysis is motivated by comments in recent theoretical and computational electrochemistry literature questioning the validity of widely assumed (local) equilibrium and the role of different timescales in the simulation of electrochemical reaction kinetics. The general argument is that because electron (ET) or proton transfer (PT) dynamics take place on attosecond or femtosecond timescales, respectively, the reaction environment should remain at least partially frozen and out of equilibrium during the reaction [2,3]. From a computational perspective this would mean that the nuclei of the reactants, solvent, and ions should not be allowed to move during a reaction and *e.g.* reorganization of the nuclei should not take place. Along these lines it has been argued that ions, presented either using continuum Poisson–Boltzmann -type models or explicit atomistic models, should not be allowed to move during the reaction [2]. Dynamics of ECIs can be described with molecular dynamics but it has recently been asserted that the solvent coordinates are "oversampled" in enhanced molecular dynamics simulations and that the solvent should appear partially frozen [4]. Besides physical arguments, simplified treatments of ECIs are often based on ice-like solvent structures and static ion environments [5]. It has also been argued that the electrode potential should not retain a constant value during a reaction event which in turn questions the application of constant potential or grand canonical ensemble (GCE) DFT methods [3].

It is certainly true that ET and PT are very fast because they generally proceed through tunneling. However, it needs to be emphasized that the processes leading to a geometry, where tunneling can take place, are substantially slower: ET and PT are generally considered activated processes [6]. For instance, general ET and PT theories consider

E-mail address: marko.m.melander@jyu.fi.

https://doi.org/10.1016/j.electacta.2023.142095
Received 15 December 2022; Received in revised form 10 February 2023; Accepted 21 February 2023
Available online 23 February 2023

that solvent or reaction medium reorganization set the relevant reaction timescale and that the reorganization energy determines the reaction barrier while the actual ET/PT step is an infinitely fast tunneling event [6]. Hence, the relevant timescale for electrochemical reactions is not determined by an ET/PT transfer event but rather the solvent or ion relaxation processes leading to a geometry where ET/PT can take place. It is not, however, *a priori* clear how slow dynamics or long timescales of the reaction environment should be considered important — are there some processes which should be considered dynamically frozen when modeling an electrochemical reaction?

More generally, the above discussion questions whether the reaction environment remains in local equilibrium during the reaction or whether some degrees of freedom are out of equilibrium on the reaction timescale. In other words, is it correct to assume that nuclear or electronic degrees of freedom react adiabatically to environment reorganization and does the environment remain in equilibrium during the reaction? In statistical mechanics these questions can be formulated in terms of ergodicity [7–9]. During an ergodic reaction, the environment is allowed to sample the entire relevant equilibrium phase space. In non-ergodic reactions some parts of the phase space are not accessible on the reaction timescale and consequently some configurations should not be included in the sampling.

Non-ergodic rate theory [7–9] provides a general framework to analyze which degrees of freedom appear dynamically frozen during a reaction. Below, I apply this theoretical machinery to analyze when and whether solvent, ion, and electron transfer dynamics remain in equilibrium during electrocatalytic reactions. This facilitates a rigorous analysis of previous arguments positing that the reaction environment should be partially frozen during an ET/PT reaction. I will show that simulations mimicking constant potential experiments in an aqueous electrolyte should treat the reaction environment dynamically and completely equilibrated unless the reaction barrier is very small (≤ 0.25 eV). For typical activated reactions, the environment must be treated in equilibrium. On the other hand, simulations of transient experiments, such as potential or current steps, should not in general allow the environment to (fully) relax and the environment dynamics need to be explicitly described.

2. Kinetics and dynamics, simulations and sampling

The present work implicitly assumes that "relevant" processes and "local" reaction environments have been appropriately chosen. Both relevance and locality depend on the time and length scale of interest. If one is interested in macroscopic electrodes used experimentally, the electric potential difference between the electrode and solvent are built during a few microseconds [10]. In this case the relevant changes in the electrostatic potential and e.g. the double layer are clearly macroscopic, and approach to equilibrium cannot be considered fast from an atomistic perspective. On such scales the electron, solvent, and ion relaxation take place simultaneously on an experimental timescale. Equilibrium is achieved only when all components of the electrochemical interface have relaxed to their equilibrium values.

In GCE-DFT and other atomistic simulations of electrochemical systems only local or microscopic equilibrium can be reached. The assumption of locality means that one is not attempting to simulate an entire dynamic, macroscopic electrochemical interface but *e.g.* a specific nuclear motion or a reaction step of interest taking place on a stable surface in the presence of chosen atoms. Furthermore, only a subset of all processes are considered "relevant" and the goal is to simulate them. The assumptions of locality and choice of relevant processes are crucial because they allow the development of hierarchical atomistic models where a fast process can be considered to be in equilibrium on the timescale of the slower processes. In turn, the slow process feels or experiences the faster process in its local equilibrium state. For example and as discussed in detail below, solvent reorganization takes place during ~10 ps whereas the number of electrons and the Fermi level (electrode potential) reach local equilibrium on a 100 fs scale. Water reorganization therefore takes place at an effectively constant Fermi level. Similarly, a reaction with a timescale longer than 100 ps experiences an effective free energy surface where the solvent is equilibriated and constant electrode potential maintained. Such assumptions on locality and relevance allow partitioning of the total system to well-defined subsystems and processes — different processes are analyzed in detail below.

2.1. Transition state theory, dynamics, and non-ergodicity

Electrochemical rate constants are almost invariably described within classical transition state theory (TST) which relies on purely statistical arguments and no dynamical quantities are present. TST assumes that a reaction $A \rightarrow B$ takes place adiabatically through a dividing surface or a transition state so that (local) thermodynamic equilibrium is maintained throughout the transition. During such an adiabatic process the entire available phase space can and should be sampled. As discussed above, the assumption of equilibrium rests on a separation of timescales since relaxation to local equilibrium within A is assumed to be faster than the $A \rightarrow B$ transition time [11]. The TST rate under constant potential conditions is obtained from grand canonical rate theory [12]

$$k_{TST} = \frac{k_B T}{h} \frac{\Xi^{\ddagger}}{\Xi^{A}} = \frac{1}{\beta h} \exp[-\beta \Delta\Omega^{\ddagger}] \tag{1}$$

where $\Xi^{\ddagger}$ and Ξ^{A} are the transition and initial state grand canonical partition functions, respectively, which are assumed fully ergodic in TST. $\Delta\Omega^{\ddagger}$ is the constant potential reaction barrier and $\beta = 1/k_B T$. The partition functions are restricted or constrained to include only the phase space (Γ_i) available to a given state i

$$\Xi^{i} = \sum_{N} \int_{\Gamma_i^N} d\Gamma \exp[-\beta(H(\Gamma^N) - \tilde{\mu}_N N)] \tag{2}$$

where Γ^N denotes the phase space available to an N-electron state and $H(\Gamma^N) = H(\mathbf{p}^N, \mathbf{q}^N)$ is the classical Hamiltonian for momenta ($\mathbf{p}^N$) and positions ($\mathbf{q}^N$).[1] $\tilde{\mu}_N$ is the chemical potential of electrons which is fixed and equal to the absolute electrode potential.

The statistical origins of TST become even more evident when the free energies are written as probabilities of being in the initial ($\rho(A)$) and at the dividing surface or the transition state ($\rho(\ddagger)$). The probabilities obey the common Gibbsian distribution where $\rho(i) = \Xi^{i}/\Xi$ with Ξ as the total partition function. Thus, the rate can be computed directly as the probability of being at the TST with a momentum in the $A \rightarrow B$ direction. This is an alternative but equivalent form of TST:

$$k_{TST} = \frac{\rho(\ddagger)}{\rho(A)} p_{A\rightarrow B} \tag{3}$$

This form explicitly tells that the TST rate constants does not depend on time or system dynamics. Furthermore, all parts of the restricted phase spaces contribute to the rate. These notions have direct consequences for the simulation of reaction rates because in a typical molecular dynamics simulation of reaction kinetics using TST, the phase space is sampled and the ergodic hypothesis is expected to hold. The ergodic hypothesis further states that time and phase space integrals yield equivalent thermodynamic expectation values. For instance, for grand free energies the ergodicity principle gives

$$\begin{aligned} \Omega_i = \langle \Omega_i \rangle &= \lim_{t\rightarrow\infty} \frac{1}{t} \int_0^t dt' \Omega_i(t') \Theta(\Gamma_i - \Gamma) \\ &= \int_{\Gamma_i} d\Gamma \rho(i) \Omega_i(\Gamma) \Theta(\Gamma_i - \Gamma) \end{aligned} \tag{4}$$

where $\Theta(\Gamma_i - \Gamma)$ enforces the sampling of phase space Γ_i and the angled brackets denote thermodynamic averages. In typical reaction kinetic

[1] A similar equation can also be derived for quantum systems [13]

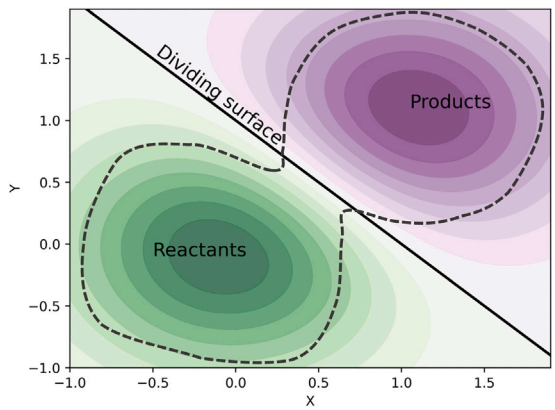

Fig. 1. Division of the X–Y phase space to ergodic and non-ergodic regions. For ergodic reactions, the initial and final states can roam the entire phase space available to them. The transition state sampling is restricted to the dividing surface. For non-ergodic reactions, only the phase space within the dashed curve can be sampled in the initial, transition, and final states.

simulations the time integral form is preferred as it allows efficient use of molecular dynamics and extraction of ensemble averages along trajectories. Long trajectories are needed to fulfill the ergodicity requirements and more through sampling of the phase space improves the accuracy of the partition functions and rates.

While TST is insensitive to timescales and dynamics, these do impact kinetics in various ways. The reaction medium may have several characteristic timescales which can be quantified using autocorrelation functions [11,15]

$$\begin{aligned} C_{AA}(t;t_0) &\equiv \langle A(t_0)A(t_0+t)\rangle_{\Gamma(t_0)} \\ &= \lim_{T\to\infty}\frac{1}{T}\int_0^T dt f(\Gamma;t_0)A(t_0)A(t_0+t) \\ &\overset{\text{eq.}}{=} \lim_{T\to\infty}\frac{1}{T}\int_0^T dt f(\Gamma;t_0=0)A(0)A(t) \\ &= \langle A(0)A(t)\rangle_\Gamma = C_{AA}(t) \end{aligned} \tag{5}$$

where $f(\Gamma;t_0)$ is the (time-dependent) phase space distribution from which the time-dependent sampling is initiated. $A(t)$ is a time-dependent quantity of interest such as dipole moment direction for rotational relaxation, position for diffusion, current for conductivity, or probability to reside either on reactant/product basins for reaction rates. Examples of different processes are shown in Fig. 2 for a solvated Pt(111) ECI. In equilibrium, denoted by "eq"., the correlation function depends only on the time difference t whereas in non-equilibrium systems also the initial time t_0 needs to be specified. In equilibrium the sampling, denoted as $\langle\rangle$, is performed from a static, time-independent phase space Γ whereas for non-equilibrium systems the sampling is taken from a time-dependent phase space distribution.

Assuming exponential decay of the timecorrelation function, a characteristic timescale τ_A is obtained from

$$M_A(t) = M_A(t=0)\exp\left(-t/\tau_A\right) \tag{6}$$

For concreteness, let us consider the impact of solvent relaxation dynamics on reaction kinetics. When the reaction barrier is very small, the timescale $\tau_k = 1/k$ for crossing the barrier region would also be very small. In such cases, the solvent reorganization time τ_r around the transition state becomes the slowest process: $\tau_r > \tau_k$, and the reaction rate is limited by the system reorganization time rather than barrier crossing as computed from TST. Theories for τ_r-limited reaction rates are most often based on Kramers' seminal work which treats the reaction event as damped diffusion along an effective reaction coordinate or the potential of mean force. The reaction rate constant is obtain by solving the (generalized) Langevin equation for a diffusion process from reactants to products across the dividing surface or transition state. The Stokes-Einstein equation further relates the diffusion coefficient to friction *i.e.* the coupling between the system dynamics along the reaction coordinate and other degrees of freedom such as solvent rotation. The theory provides a stochastic description of reactive trajectories crossing the dividing surface (see Fig. 1) with multiple barrier recrossings. Alternatively, the theory can be seen to describe the impact of medium relaxation time (e.g. solvent rotation or reorganization time τ_r) on the reaction rate [16,17].

Following Kramers' ideas, the theoretical foundations of dynamic solvent effects on electrochemical and electron transfer reactions were developed in the 1970s and 1980s [18]. While theories of varying complexity were developed to capture the impact of τ_r on reaction kinetics, in all these theories τ_r impacts only the *prefactor* while the reaction barrier remains unaltered [6,19]. Hence, the reorganization dynamics and timescale can be added as a prefactor correction to an otherwise ergodic TST rate expression,

$$k^{dyn}_{TST}(\tau_r) = \frac{f(\tau_r)}{\beta h}\frac{\Xi^\ddagger}{\Xi^A} \tag{7}$$

with a generic function f to describe the impact of relaxation dynamics. It needs to be re-emphasized that even here, the system is to assumed fully ergodic. While the ergodic hypothesis seems deeply ingrained in chemical kinetics, it does bring forth the issue of timescales. For instance, condensed matter and electrochemical reactions typically have several timescales from sub-femtosecond electron motion to bond vibrations on the femtosecond scale, picosecond solvent reorganization, or double layer dynamics on the microsecond scale as inferred from impedance spectroscopy. In a strict TST perspective all these timescales contribute to the partition functions, barrier, and kinetics, and should therefore be included. While this is clearly impossible in practical simulations, it is not at all clear *which timescales are relevant to the reaction kinetics* and should be included in the simulation of reaction rates. In other words, when is departure from ergodicity acceptable and which timescales or processes are relevant to reaction kinetics? Should some motions or degrees appear frozen on the timescale of an electrochemical reaction?

This question has been analyzed only recently by Matyushov in a series of works leading to the development of non-ergodic rate theory [7–9]. While originally developed for protein electrochemistry, the formalism is applicable more generally and also to ECIs. The key insight of this theory is that some motions and degrees of freedom appear dynamically frozen at the timescale of a reactive event. This leads to *ergodicity breaking and has a direct impact on the reaction barrier* since the *barrier* becomes a function of system dynamics. Qualitatively, this means that the system does not have time to roam the entire phase space on the reaction timescale as depicted in Fig. 1. More quantitatively, the system dynamics taking place on a timescale (τ_s) longer than the reaction itself become dynamically frozen when $\tau_s > \tau_k$. Hence, non-ergodicity becomes a relevant factor when $k\tau_s > 1$ and the contributions from dynamic processes taking place on $\tau_s > \tau_k$ timescales should be omitted.

Non-ergodicity places restrictions on which regions of the phase space contribute to the partition function and reaction barrier as depicted in Fig. 1. In particular, non-ergodicity dictates that the phase space averages and sampling times should be limited to regions fulfilling the $\tau_s > \tau_k$ condition. For the grand canonical free energy this is enforced by constraining the phase space sampling as

$$\begin{aligned} \Omega_i(\tau_s) = \langle\Omega_i\rangle_{\tau_s} &= \lim_{t\to\tau_s}\frac{1}{\tau_s}\int_0^t dt'\Omega_i(t')\Theta(\Gamma_i-\Gamma) \\ &= \int_{\tau_s k<1} d\Gamma\rho(i)\Omega_i(\Gamma) \end{aligned} \tag{8}$$

This equation tells that the system dynamics contribute to *both* the prefactor and the barrier. The resulting equation is called the non-ergodic TST (ne-TST):

$$k^{dyn}_{ne-TST}(\tau_r,\tau_s) = \frac{f(\tau_r)}{\beta h}\frac{\Xi^\ddagger(\tau_s)}{\Xi^A(\tau_s)} \tag{9}$$

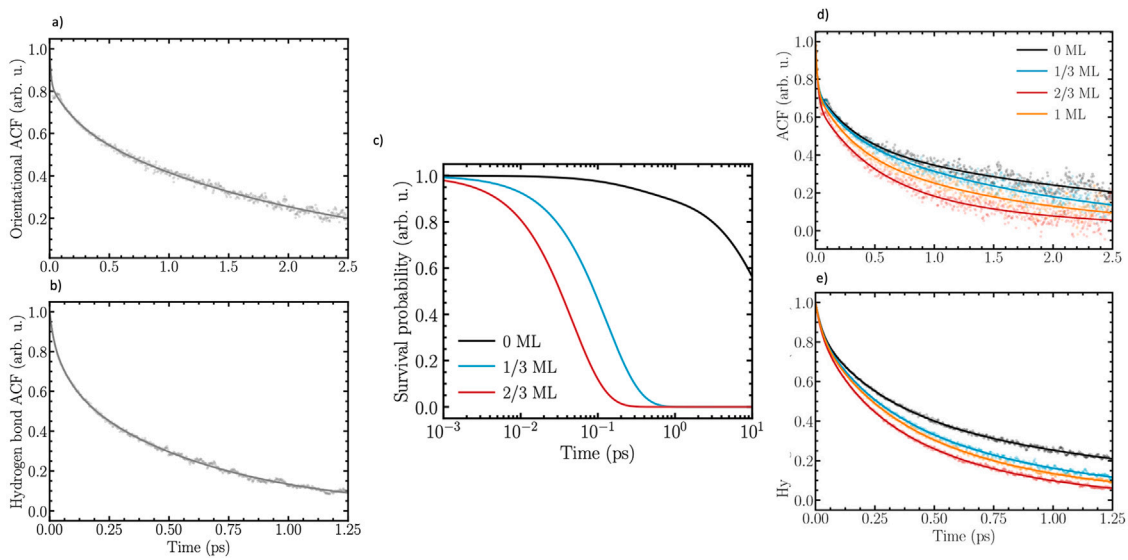

Fig. 2. (a) Orientational and (b) hydrogen bond time correlation for bulk water. (c) Survival properties of adsorbed water on Pt(111) as a function of hydrogen coverage. (d) Orientational and (e) hydrogen bond time correlation for adsorbed water.
Source: Reproduced with permission from Ref. [14].

Unlike k_{TST} or k_{TST}^{dyn}, the *barrier* of k_{ne-TST}^{dyn} depends on system dynamics through τ_s. The previous equation should be solved self-consistently or iteratively to satisfy $\tau_s > \tau_k$ to correctly sample the partition functions. Also note that in the grand canonical picture of electrochemical rates, the partition functions depend explicitly on the electrode potential through the constant electron electrochemical potential.

The iterative nature and electrode potential-dependency make the previous equation very difficult to solve. Below I focus on a simpler task and discuss in detail whether and when non-ergodicity should be accounted for in the atomic-scale simulation of electrochemical reaction rates. The main goal is to analyze which solvent, electrolyte, and electron transfer processes should contribute to electrochemical kinetics in aqueous electrolytes. I will first discuss the equilibrium case where the electrode potential is kept constant and the grand canonical ensemble for the electrons is valid. This is the appropriate framework for constant potential electrolysis or cyclic voltammetry with slow potential ramping. Finally, I address electronic transients, where the electrode potential is suddenly changed as experimentally realized in potential step methods.

2.2. Solvent

There are three main methodological approaches to modeling the solvent at ECIs: microsolvation with a frozen solvent environment, time-averages from molecular dynamics, or phase space averages used in implicit solvation models such as dielectric continuum or statistical liquid state theories [1,5]. A recent work argued that enhanced molecular dynamics simulations can potentially "oversample" the phase space as all points along the reaction pathway are sampled for extended periods of time [4]. The argument is that the ET and PT takes place instantaneously when the transition state is reached and hence the barrier region should be considered non-ergodic with a (partially) frozen environment. The extreme case of non-ergodicity would then be the frozen microsolvation method where the solvent would be completely frozen on the reaction timescale. Implicit solvation models present the other extreme and correspond to the situation where the entire solvent is ergodic and remains in (local) equilibrium at all points along the reaction coordinate. Besides simulations, it has been recently suggested that electrocatalytic reactions such as alkaline hydrogen evolution might be controlled by double layer rigidity [20] which can be understood in several ways: for small barriers the solvent relaxation time τ_r might control reaction kinetics, the solvent might appear frozen and non-ergodic on the reaction timescale, or the rigidity impacts reaction time τ_k which would correspond to a larger solvent reorganization energy and higher reaction barrier.

Non-ergodic rate theory can be used to answer whether a typical solvent, such as water, should be considered frozen during an elementary reaction. For this it is beneficial to cast the phase space in the frequency domain through a Fourier transform. The phase space becomes $d\Gamma = \Pi_\omega \Pi_i dq_i(\omega) dp_i(\omega)$ and only frequencies higher than the reaction rate or frequency are considered. Hence, only sufficiently high-frequency motions of the environment contribute to the rate and free energies are accordingly sampled with the constraint $\omega_k \geq \tau_k$:

$$\Omega_i(\omega_k) = \int_{\Gamma_i} \rho(i)\Omega_i(\Gamma)\Pi_{\omega_k > \tau_k} \Pi_i dq_i(\omega) dp_i(\omega) \tag{10}$$

For water, the relevant timescales are the vibrational, rotational, and translational or librational times which can be either measured or simulated. As the current interest is on reactions take place at or near the electrode, simulated values are used since these offer very high spatial resolution of the ECI not achieved in experimentally. The relevant timescales can then be computed from vibrational or velocity, rotational, and translational time-correlation functions. Typical time-correlation functions for water near Pt(111) are shown Fig. 2. These time-correlation functions demonstrate that both in bulk and close to the rather strongly binding Pt(111) surface the water reorganization, vibrational, and librational time constants are $\tau_s^{rot} \approx 5$ ps, $\tau_s^{vib} \approx 1$ ps, and $\tau_s^{lib} \approx 20$ps, respectively. Even the slowest motion, water libration, can be considered fast. The criterion in Eq. (8) for a reaction entering non-ergodic region in water is computed from the $\tau_s > \tau_k$ condition: $\tau_s^{lib} k \leq 1 \rightarrow k \leq 1/\tau_s^{lib} \rightarrow 1/h\beta \exp[-\beta \Delta\Omega^{\ddagger}] \leq 1/\tau_s^{lib} \rightarrow \Delta\Omega^{\ddagger} < 0.25$ eV. Put otherwise, the reaction barrier at room temperature should be smaller than 0.25 eV for water non-ergodicity to contribute even on the strongly binding pristine Pt(111) surface.

It is therefore rather safe to conclude that water should appear completely ergodic and mobile on the timescale of a typical activated electrochemical reaction; simulations should be allowed to sample the entire phase space along the reaction pathway. There is very little risk or possibility of oversampling water in enhanced sampling MD simulations. The implicit continuum models capture this physical situation

correctly whereas ice-like overlayers or static water molecules do not. If static water models are used, at least the vibrational, rotational, and translational partition functions should be evaluated to estimate the corresponding contributions to free energies.

Besides simulations, the above analysis has some direct consequences on understanding the origin and impact of the suggested interfacial water rigidity in alkaline HER. Unless extremely small barriers (<0.25 eV) are expected, water appears completely mobile and dynamic in alkaline HER. For such small barriers, the slowest timescale would no longer be barrier crossing but water relaxation dynamics for which the slowest component is $\tau_s^{lib} \sim 20$ ps corresponding to an effective barrier of ~0.25 eV which can still be consider fairly small. This indicates that water reorganization dynamics are not the origin of the suspected rigidity. An alternative perspective was offered by Huang et al. [21] who included *rigidity as an energetic parameter* in a model Hamiltonian framework to address local water (reorganization) *thermodynamics* rather than its dynamics. Recent simulations also support the perspective that interfacial rigidity is related to hydrogen bonding network and thermodynamics rather dynamics [22]. The above analysis on water reorganization timescales and ergodicity supports this energetic rigidity interpretation as water at the interface appears highly dynamic but the reorganization energy may be affected by high interfacial electric fields or chemical interactions.

2.3. Electrolyte

This section discusses electrolyte dynamics under constant electrode potential conditions without any notable transients which are to be discussed in subsequent sections. As such, the question addressed here is different from Refs. [3] or [23] treating the ion dynamics *after* instantaneous electron transfer — these studies correspond to transient experiments. This section considers whether the electrolyte ions should appear completely mobile *during* an elementary reaction step where the electrode charge may change but its potential remains constant — these correspond to steady-state experiments. The main goal here is to answer whether an instantaneous ion redistribution or frozen ion treatment is more appropriate. In other words, we consider times scales at which ions move during the reaction, and in particular whether the electrolyte ions should be considered non-ergodic or frozen on the timescale of an elementary reaction step. This is an important consideration to establish the validity explicit ion simulations and implicit Poisson–Boltzmann -type electrolyte models which treat ions fully equilibrated.

The treatment below is restricted to simple but widely used inorganic electrolytes, and organic electrolytes or ionic liquids are not consider. It has already been shown that *e.g.* ionic liquid electrolytes are prone to non-ergodicity and appear at least partially frozen [8]. Compared to these complex electrolytes, dynamics of simple electrolytes are mostly related to their translational motion. Ion dynamics can then be described using their conductivities which are available from the current or velocity autocorrelation functions [24,25] or experiments. Conductivity, in turn, defines ion mobility [26]. In dilute electrolytes, the ion dynamics can be treated with the Nernst–Planck equation which accounts for diffusion, electromigration, and convection [26]. While convection is important in bulk electrolyte, near an interface the fluid flow is greatly diminished and typically non-slip boundary conditions are applied even for hydrodynamic simulations. It is therefore assumed that convection can be neglected in the below analysis of interfacial electrochemical kinetics. Within these limitations, ion dynamics and electrolyte relaxation times can be quantified using the Nernst–Planck equation for ion diffusion and migration fluxes (J). The flux is directly proportional to ion mobility and the gradient of ion electrochemical potential ($\tilde{\mu}_i$)

$$\frac{\partial c_i(x,t)}{\partial t} = -\nabla \cdot J_i = -\nabla \cdot [-M_i c_i(x,t) \nabla \tilde{\mu}_i(x,t)] \tag{11}$$

where $c_i(x,t)$ is the time-dependent spatial concentration of i and M_i is the corresponding mobility. The previous equation shows that ion dynamics can be treated using a generalized diffusion equation. Even more generally, the diffusion equation can be extended to include free energy barriers using non-equilibrium thermodynamics [27] or concentrated solution theory [28]. This is beneficial for the description of (partial) ion desolvation taking place *e.g.* during specific adsorption or ion-coupled ET/PT reactions. The effective rate for the total ion flux can be written as

$$k_i^{el}(x) = k_i^{0,el} \exp\left[-\beta\left(\tilde{\mu}_i^{\ddagger}(x) - \tilde{\mu}_i^0\right)\right] \tag{12}$$

where $\tilde{\mu}_i^{\ddagger}(x)$ is the spatially varying electrochemical barrier for ion movement while $\tilde{\mu}_i^0$ is the corresponding bulk value. The prefactor k_i^0 is the bulk ion transfer rate related to ion mobility as

$$k_i^{0,el} = \frac{M_i c^0 dydz}{dx} \tag{13}$$

where c^0 is the standard state concentration and $dx/dydz$ denotes space discretization.

After establishing an effective rate expression for electrolyte dynamics, the impact of ion mobility on reaction rate constant is addressed. The total apparent rate constant (k_{app}) depends on both the electrocatalytic reaction (k_{ec}), which is a function local ion concentration $c(x)$, and the electrolyte dynamics $k_i^{el}(x)$. When both contributions are included, k_{app} is analogous to the rate constant of partially diffusion-controlled reactions

$$\frac{1}{k_{app}(x)} = \frac{1}{k_{ec}(c(x))} + \frac{1}{k_i^{el}(x)} \tag{14}$$

which is directly related to the timescale of electrolyte transfer: $\tau_{el}(x) = k_{app}(x)^{-1}$. The previous equation can be rigorously derived from *e.g.* the stable states picture [29] or as a stationary limit for diffusion-influenced reaction rates [30–32]. For explicitly time-dependent reactions, a similar expression can be derived from a generalized Smoluchovski equation [33,34].

In bulk electrolyte the diffusion coefficients are ~0.1 Å^2 /ps or 10^{-5} cm^2/s in more conventional units [2]. One Å^2 ion "hop" or movement corresponds to a hopping rate constant of $k_i^{0,el} \approx 10^{11}\text{s}^{-1}$ for 1 molar solution and can be considered faster than most electrocatalytic reactions. Alternatively, the electrochemical effective diffusion constant can be analytically estimated from the double layer charging time as $\tau_{EDL} = \lambda_D * L/D^2$, with λ_D being the Debye length, L the thickness of the diffusion layer, and D diffusion coefficient [10]. An ion would then traverse across a typical DFT simulation cell of 10 × 10 Å, with a rate $k_i^{0,el} \approx 10^9\text{s}^{-1}$. Hence, the diffuse double layer, where free diffusion and migration take place, treated in a typical DFT simulation relaxes on a nanosecond (10^9s^{-1}) timescale corresponding to an effective electrolyte mobility barrier of ~ 0.2 eV.

When an ion approaches the surface and becomes quasi-specifically adsorbed, it partially loses its solvation shell. This causes an additional locally varying barrier for ion transfer. These barriers depend on the ion, surface, and the electrode potential and are not widely available for different combinations but Schmickler et al. [35] recently evaluated these systematically for monovalent ions at a gold–water interface. They found the desolvation barriers to be 0.1–0.3 eV which means that the local cation transfer rate $k_i^{el}(x)$ for a 1 Å hop varies between 10^8 s^{-1} and 10^5 s^{-1} or $\tau_{el} \sim 10$ ns and $\tau_{el} \sim 0.1$ µs, respectively. With these values one can study the apparent rate constant from Eq. (14) for a range of effective ion transfer barriers as shown in Fig. 3. This figure clearly shows that the impact of electrolyte mobility on the overall rate depends sensitively on the intrinsic reaction rate, k_{ec}.

Two particular examples are considered in more detail: (i) a surface reaction where both the initial and final states are adsorbed and (ii) approach or adsorption of a molecule to a surface from the liquid phase while electron transfer takes place. Type (i) is the most common electrocatalytic reaction treated with DFT methods. Type (ii) reactions

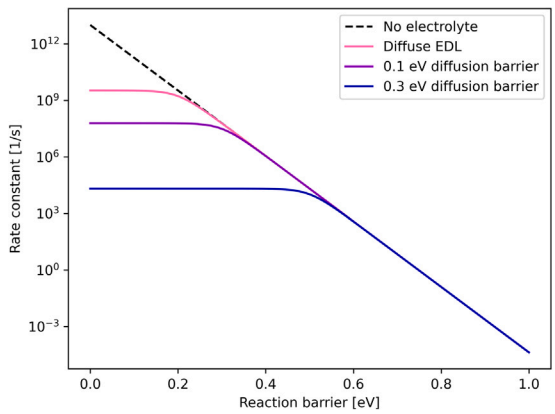

Fig. 3. k_{app} as a function of the reaction free energy barrier without ions, ions in the diffuse layer, and for mobilities with two different ion diffusion barriers at room temperature.

are relevant for *e.g.* CO_2 or O_2 adsorption processes where a molecule travels from a bulk solution to an interface. Recent studies show that such reactions are often accompanied by charge transfer and can be coupled to ion transfer [36,37]. For option (ii), two distinct cases emerge: either ions remain in the inner- or outer-Helmholtz regions throughout the adsorption/charge transfer process or they travel with the reacting molecule from the bulk solution to the inner-Helmholtz layer. In the former case no ion solvation–desolvation processes are expected whereas in the latter desolvation may take place.

In both (i) and (ii) reaction types the ions can be treated in two different ways: quasi-specifically adsorbed and partially desolvated ion need to be treated explicitly while non-adsorbed ions in the diffuse double layer can be described using either explicit or continuum models. The adsorbed ions are usually kept frozen or allowed to move only at the surface. The above discussion on adsorption/desorption barriers and the results in Fig. 3 demonstrate that freezing the adsorbed ions is a reasonable approximation if the reaction barrier is smaller than 0.4–0.6 eV. For higher barriers, even adsorbed ions should be allowed to desorb and ion exchange between the inner- and outer-Helmholtz layers with the corresponding solvation–desolvation processes should be permitted.

Electrolytes in the diffuse or outer-Helmholtz double layer do not undergo desolvation processes and are significantly more mobile than the adsorbed ions. As discussed above, the diffuse double layer of a typical DFT simulation cell is expected to completely reorganize on a sub-nanosecond timescale. This claim is supported by the analysis of the analytical double layer charging time estimate $\tau_{EDL} = \lambda_D * L/D^2$ [10]. $\tau_{EDL} \approx 10$ ms under typical experimental conditions meaning that the electrochemical double is out of equilibrium on the macroscopic scale. However, on the length scale of typical DFT calculations (~10 Å), τ_{EDL} is in the sub-ns times scale. Fig. 3 shows that the double layer diffusion limitations are important only when the reaction barrier is smaller than ~ 0.25 eV which corresponds to very fast reactions at room temperature. Hence, unlike concluded in Ref. [2], *ions in the diffuse double layer should be allowed to completely relax when simulating the reaction barrier of an activated process — based on non-ergodic rate theory and diffusion timescales the nuclear, electronic, and ionic motion associated with reaction events should adiabatically follow medium reorganization unless the reaction barrier is very small.*

The above conclusion has a direct impact on how electrolyte effects should be simulated. Especially related to the CO_2 reduction reaction, electrolyte effects are often explained in terms of a local electric field which at the DFT-level is often evaluated from a single frozen configuration where an ion is in the electrolyte near a reactant [38]. Naturally, a large electric field is generated around the frozen ion. This can be easily understood using a simple image charge picture [39] which affords an analytic formula for the electric field (F) generated by an ion with charge Q at distance r from the surface:

$$F(r,a) = \left[\frac{Q}{2\pi\epsilon\left(r^2+a^2\right)}\right]\left[\frac{r}{\sqrt{r^2+a^2}}\right] \tag{15}$$

with an offset a measured along the surface between the ion and reactant position, where the field is measured (see Fig. 4).[2] The image charge picture shows that when the ion is right above the reactant, e.g. CO_2, $a = 0$ and reactant feels a very high electric field. This is in a very good qualitative agreement with the static DFT simulations of electrolyte effects [38]. The field, however, decreases very quickly when the ion is displaced away from the reactant as shown in Fig. 4. Furthermore, accounting for ion mobility in the diffuse double layer drastically changes the field felt by the reactant. The thermodynamically relevant field generated by a mobile ion is obtained by averaging the field along the simulation cell a-coordinate:

$$\langle F(r)\rangle = \frac{1}{L}\int_0^L F(r,a)da = \frac{Q}{2\pi\epsilon}\left(\frac{1}{r\sqrt{L^2+r^2}}\right) \tag{16}$$

L could be computed from the local ion concentration as the mean average distance between the ions. As an example, we consider a typical DFT simulation setup consisting of a 3 × 3 surface unit cell $L \approx 8$Å and a single mobile ion. For such a system the resulting average field is vanishingly small as can be seen from Fig. 4. The results from this simple image charge approach show that the local field is very weak if the ion is treated as a mobile, diffusing particle; as discussed, this is the relevant situation for most activated electrocatalytic reactions if explicit ion adsorption does not take place.

If the ion and reactant interact strongly, the above integral needs to be modified to include the ion-reactant probability distribution function when computing the average value. The local field effects are notable only if a frozen ion configuration on top of the reactant can be justified — this situation can arise when the reactant and ion form *e.g.* coordination complexes [37] but even then direct (chemical) interactions are expected to be more dominant than field effects. This conclusion is supported by recent theoretical works of the oxygen evolution [40] and CO_2 reduction [41] reactions for which the electrostatic or electric field effects were shown to be minor.

2.4. Electron conductivity limitations

Compared to reaction rate theories in the canonical, constant charge ensemble, the grand canonical rate theory in Eqs. (1)–(2), [12] requires that also the number of electrons responds very quickly to changes in the system. From the perspective of non-ergodic rate theory, this requirement is satisfied when the electron transfer within the electrode is faster than the reaction or any relevant reorganization processes. Consequently, the electrode potential should be kept constant only when electron transfer within the electrode is the fastest process in the studied system. This means that the number of electrons must adiabatically react to all *relevant* nuclear rearrangements. Below, I test when the constant electrode potential treatment is valid and when electron transfer rate within the electrode can be assumed adiabatic on the reaction timescale. This analysis presents a new dimension to both non-ergodic and grand canonical rate theories.

The conductivity of metallic electrodes is very high, on the order of 10^5 S/cm [42]. The effective electron diffusion constant can be computed from conductivity and the number of states at the Fermi-level: [43] the effective diffusion coefficient for electrons in metallic electrodes is at least 1 cm^2/s, that is $D_{eff} > 10^5$Å^2/ps, [43] which

[2] The electrostatic potential due to the electrode generates an additional electrostatic field ($V(r)$) which would modify the field to $F'(r,a) = F(r,a) - \frac{\partial V(r)}{\partial r}$. Here the impact of $V(r)$ is neglected as it is not strictly related to ion effects.

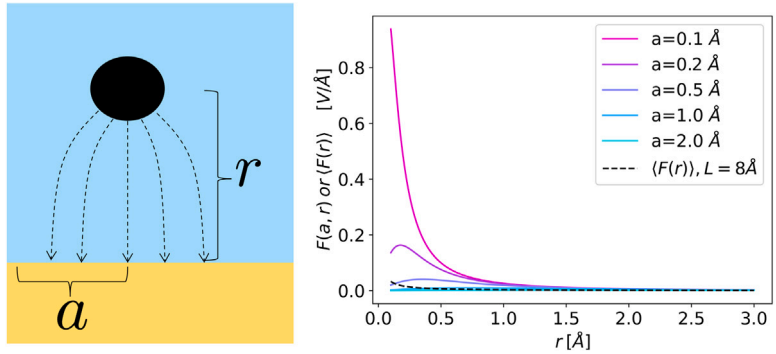

Fig. 4. Left: Schematic of the electric field created by an ion at an interface. Right: The field as a function of distance from surface (r) and the offset along the surface (a) computed from Eq. (15). The ion charge is +1 and the interfacial dielectric constant is 6.

is around six orders of magnitudes larger than the ion diffusion coefficient. The electron transfer within metals is therefore significantly faster than any relevant reaction and the number of electrons can be treated adiabatically in constant potential calculations. Hence, Eqs. (1)–(2) can be reliably applied to compute reaction rates at fixed electrode potentials.

Semiconducting electrodes are notably more challenging as the conductivity depends on several factors such as electronic structure, intrinsic charge transfer dynamics such as hole/electron hopping rate, semiconductor thickness, and the number of charge carriers. The intrinsic charge transfer rate is quantified by charge carrier mobility which for typical semiconductor electrodes varies in the range of 10^2–10^4 $cm^2V^{-1}s^{-1}$ [44]. While these charge mobilities are higher than electrolyte mobilities, [44] the low number of carriers limits semiconductor conductivity. Experimentally, the low semiconductor conductivity manifests as a inseparability of Faradaic (reaction) and semiconductor charging currents [45,46].

In what follows, it is assumed that carrier diffusion takes place through polaronic conduction which is relevant for *e.g.* TiO_2, CeO_2, GaAs, and Fe_2O_3 electrodes. This assumption does not invalidate the generality of the analysis but makes quantification easier because carrier diffusion constants can be used to quantify the relevant timescale for charge transfer dynamics in complete analogy to electrolyte mobility. In general, the diffusion coefficient (D) is related to conductivity (σ) and mobility (ν) through [44,47]

$$\sigma = q\nu = q\beta D = q\beta R^2 k_{ct} \tag{17}$$

where q is the carrier charge, R the hopping distance, and k_{ct} the charge transfer coefficient and the elementary charge is taken as unity. The electron diffusion coefficients vary significantly across different materials. For CeO_2, [48] α-Fe_2O_3, [49], and Ta_3N_5 [50] the electron polaron diffusion coefficients are $\sim 3 \times 10^{-4}$ cm^2/s, $\sim 10^{-4}$ cm^2/s, and $\sim 2 \times 10^{-5}$ cm^2/s respectively. For anatase TiO_2, the effective electron diffusion constant is $> 10^{-2}$ cm^2/s but both the carrier concentration and temperature affect mobility and conduction mechanism [51]. The overall conductivity is determined by the competition between band and polaron conduction mechanisms, and polaron conductivity is expected to provide a lower bound for electron conductivity or diffusion at room temperature.

The question whether the electrode potential should remain constant when simulating semiconductor electrodes cannot be answered with complete certainty: due to material and carrier concentration effects, a general conclusion cannot be given. However, the above values for effective electron diffusion coefficients for a range of relevant semiconductor electrodes are of similar magnitude or higher than bulk electrolyte diffusion coefficients [2]. In analogy to electrolyte diffusion timescales, the electrons in relevant semiconductor electrodes move as fast as or faster than electrolyte ions. This is consistent with the approximation by Bisquert [52] showing that even in a poorly conducting semiconductor electrode ($\nu \sim 10^{-2}$ cm^2/Vs) charge transfer across a 50 nm nanoparticle occurs in $\sim$ 100 ps. These estimates imply that even in semiconductor electrode simulations the electrode potential should be kept fixed if the studied reaction is an activated process with a barrier higher than ~0.2–0.3 eV.

2.5. Non-equilibrium effects and transients

While the previous sections assumed the system to be under constant potential conditions, here the focus is shifted to non-equilibrium systems where either the electrode potential or charge is rapidly changed. Such sudden changes lead to transient behavior as the system relaxes to a new equilibrium state. The relaxation dynamics and correlation functions in such systems depend on time t_0 in contrast to equilibrium systems where only time differences are important (see Eq. (5)). In contrast to equilibrium systems, non-equilibrium partition functions, correlation functions, dynamics, etc. depend explicitly on time.

For concreteness, one can consider an electrode potential step experiment. The initial state is taken from the equilibrium phase space distribution corresponding to the electrode potential U_0 at $t_0 = 0$. At $t_0 = 0$, the potential is suddenly changed to a new value U_1 and the system now evolves on the space phase belonging to U_1. In an equilibrium system only the phase space available at U_0 would be explored. This indicates that the simulation or experimental interpretation of equilibrium and non-equilibrium quantities need to differ. In general, the crucial difference between equilibrium and transient simulations is the way the system is prepared and sampled. The rates of an equilibrium system can be quantified from (non-ergodic) statistical properties using Eq. (9). But in a non-equilibrium system only the initial state is probed statistically while the reaction is initiated by a non-adiabatic charge or potential step after which the reaction rates need to be computed from dynamic trajectories initiated from the initial equilibrium state according to Eq. (5).

The atomic scale simulation of electrochemical reaction kinetics in transient systems remains practically unexplored. Very recently, Schmickler and Santos simulated hydrogen desorption from graphene to water following sudden charge injection [3]. It was observed that hydrogen desorption following positive charge injection is almost immediate and takes place within a picosecond; the reaction is much faster than water rotation, diffusion, or libration and takes place under both non-equilibrium and non-ergodic conditions. The system does not have time to relax to any new equilibrium state before the reaction takes place. Accordingly, Schmickler and Santos highlight that the "reaction experiences the local field, not the thermodynamic average" [3]. The studied desorption step clearly takes place under non-equilibrium conditions and explicit simulation of system dynamics and relaxation are required. Note that to obtain a thermodynamically consistent view of the desorption time, the simulations should be initiated and propagated from different initial conditions according to Eq. (5).

The fast hydrogen desorption provides an extreme example of a reaction that is much faster than solvent relaxation and is even potentially limited by electrode conductivity. The relevant dynamic quantities for describing such sudden reactions are the relaxation timescales following charge injection. For the double layer relaxation, i.e. solvent and electrolyte dynamics, the timescale can be inferred from the simulations of outer-sphere electron transfer on a metallic electrode [23]. Depending on the surface charge and electrolyte concentration, the double layer relaxation time varies in the range 50–400 ps which is clearly slower than the hydrogen desorption. These values are close to the estimates for electrolyte relaxation evaluated from the quasi-free diffusion model treated in a previous section where it was shown that a ∼ 10 Å displacement of non-adsorbed ion the double layer takes place on a ∼1 ns timescale. Fig. 3 further shows that diffusive relaxation times longer than ∼1 ns start to limit the reaction rate when the barrier is below 0.2 eV. If the reaction is faster than solvent or electrolyte relaxation, the reaction rate cannot be estimated without explicit simulation of dynamics leading to a reactive event. In such cases, the reaction appears to be basically barrierless and transition state theory cannot be utilized. Instead, approaches based on diffusive dynamics, such as Kramers' theory discussed above, should be considered.

Compared to the solvent and ions relaxation, electron and electrode potential relaxation in metals is much faster than that of the double layer. For instance, a recent study modeled electron or potentiostat relaxation with a 100fs timescale [53] which is close to the charge relaxation of graphene during hydrogen desorption [3]. Hence, in ultrafast non-equilibrium reactions taking place on ∼100fs timescales even the electrode potential appears to be out of equilibrium and constant potential calculations should not be used. Furthermore, in such fast reactions the electron motion appears to take place on the same timescale as nuclear motion and the two cannot be fully separated: in such cases, one should account for electronic non-adiabaticity using an explicit evolution of both the electron and nuclear degrees of freedom using *e.g.* Ehrenfest dynamics [54].

3. Discussion and conclusions

The theory and simulation of electrochemical and electrocatalytic kinetics has been built around transition state theory which assumes the system be and remain in (local) equilibrium and that system dynamics do not impact reaction rates. In recent literature this premise has been questioned. It has been purported that the reaction environment, *i.e.* the solvent and electrolyte, should remain frozen and unequilibrated during electrochemical ET and PT steps. In similar vein, it has been questioned whether the electrode potential should be kept fixed when simulating reaction kinetics. This is a crucial question for constant potential or grand canonical ensemble simulations which require the electric conductivity to be fast compared to all other system timescales. As these viewpoints question the applicability of most theoretical and simulation approaches developed and used to study electrochemical reaction rates, their validity needs careful assessment. In this critical review, I have reviewed and re-analyzed these claims from the perspective of non-ergodic rate theory which provides a rigorous framework to study when or whether the reaction environment should appear frozen.

The analysis shows that in most activated electrochemical reactions with a barrier higher than 0.2–0.3 eV, *the reaction environment is completely mobile and equilibrated under constant potential conditions in water.* This finding strongly supports that the ergodicity and adiabaticity assumptions of transition state theory are valid in typical electrochemical and electrocatalytic reactions in aqueous electrolytes; both water and ions should be treated as (locally) equilibriated and mobile. For comparison, the small reaction barriers of 0.2–0.3 eV correspond to ∼ 0.8–1.2 eV reorganization energies typical for small redox couples in water. However, for larger solutes and more complex, such as ionic liquids, the reorganization energy can be as small as 0.3 eV [55] and non-ergodic effects are expected to be more prominent than for small molecules in water. For both metallic and relevant semiconductors electrodes the impact of electrode conductivity is minimal and constant potential calculations within GCE-DFT offer reliable representation of constant potential experiments. Only for ultrafast reactions or transient methods should the environment be considered (partly) frozen and out of equilibrium.

The simulations and theory of electrochemical reactions under fixed potential conditions should therefore treat an aqueous electrolyte completely dynamically and the electrode potential strictly constant (apart from fluctuations due to the fluctuation–dissipation theorem). Hence, enhanced sampling simulations cannot oversample water or ion configuration space, and longer sampling will improve the accuracy of reaction rate estimates. This also means that the local equilibrium assumption of implicit solvent or electrolyte models, such as Poisson–Boltzmann methods, is correct and that insight from frozen water/ion calculations should be approached cautiously. These perspectives also highlight the necessity of treating solvent/electrolyte reorganization under fixed electrode potential conditions. Hence, approaches such as diabatic model Hamiltonians [6,56] or valence bond -based electrochemical reaction rate theories [1,12] highlighting the role of reorganization are expected to become increasingly more important and applicable to electrochemical kinetics.

Declaration of competing interest

The authors declare the following financial interests/personal relationships which may be considered as potential competing interests: Marko M. Melander reports financial support was provided by Academy of Finland.

Data availability

No data was used for the research described in the article.

Acknowledgments

The Academy of Finland funding through the CompEL, Finland project (#338228) is gratefully acknowledged.

References

[1] F. Domínguez-Flores, M.M. Melander, Electrocatalytic rate constants from DFT simulations and theoretical models: Learning from each other, Curr. Opin. Electrochem. 36 (2022) 101110.

[2] J.A. Gauthier, S. Ringe, C.F. Dickens, A.J. Garza, A.T. Bell, M. Head-Gordon, J.K. Nørskov, K. Chan, Challenges in modeling electrochemical reaction energetics with polarizable continuum models, ACS Catal. 9 (2) (2019) 920–931, http://dx.doi.org/10.1021/acscatal.8b02793, https://doi.org/10.1021/acscatal.8b02793.

[3] W. Schmickler, E. Santos, Desorption of hydrogen from graphene induced by charge injection, Chem. Electro. Chem. 9 (16) (2022) e202200511, https://doi.org/10.1002/celc.202200511, URL https://chemistry-europe.onlinelibrary.wiley.com/doi/abs/10.1002/celc.202200511.

[4] R. Kronberg, K. Laasonen, Reconciling the experimental and computational hydrogen evolution activities of pt(111) through DFT-based constrained MD simulations, ACS Catal. 11 (13) (2021) 8062–8078, http://dx.doi.org/10.1021/acscatal.1c00538, https://doi.org/10.1021/acscatal.1c00538.

[5] R. Jinnouchi, K. Kodama, Y. Morimoto, Electronic structure calculations on electrolyte–electrode interfaces: Successes and limitations, Curr. Opin. Electrochem. 8 (2018) 103–109.

[6] R.E. Warburton, A.V. Soudackov, S. Hammes-Schiffer, Theoretical modeling of electrochemical proton-coupled electron transfer, Chem. Rev. 122 (12) (2022) 10599–10650, pMID: 35230812, http://dx.doi.org/10.1021/acs.chemrev.1c00929, https://doi.org/10.1021/acs.chemrev.1c00929.

[7] D.V. Matyushov, Protein electron transfer: Dynamics and statistics, J. Chem. Phys. 139 (2) (2013) 025102, http://dx.doi.org/10.1063/1.4812788, https://doi.org/10.1063/1.4812788.

[8] D.V. Matyushov, M.D. Newton, Electrode reactions in slowly relaxing media, J. Chem. Phys. 147 (19) (2017) 194506, http://dx.doi.org/10.1063/1.5003022, https://doi.org/10.1063/1.5003022.

[9] D.V. Matyushov, Protein electron transfer: is biology (thermo)dynamic? J. Phys.: Condens. Matter 27 (47) (2015) 473001, http://dx.doi.org/10.1088/0953-8984/27/47/473001, https://doi.org/10.1088/0953-8984/27/47/473001.

[10] J. Huang, On obtaining double-layer capacitance and potential of zero charge from voltammetry, J. Electroanal. Soc. 870 (2020) 114243.

[11] R. Zwanzing, Nonequilibrium Statistical Mechanics, Oxford University Press, 2001.

[12] M.M. Melander, Grand canonical rate theory for electrochemical and electrocatalytic systems I: General formulation and proton-coupled electron transfer reactions, J. Electrochem. Soc. 167 (11) (2020) 116518, http://dx.doi.org/10.1149/1945-7111/aba54b, https://doi.org/10.1149/1945-7111/aba54b.

[13] M.M. Melander, M.J. Kuisma, T.E.K. Christensen, K. Honkala, Grand-canonical approach to density functional theory of electrocatalytic systems: Thermodynamics of solid-liquid interfaces at constant ion and electrode potentials, J. Chem. Phys. 150 (4) (2019) 041706, http://dx.doi.org/10.1063/1.5047829, https://doi.org/10.1063/1.5047829.

[14] R. Kronberg, K. Laasonen, Coupling surface coverage and electrostatic effects on the interfacial adlayer–water structure of hydrogenated single-crystal platinum electrodes, J. Phys. Chem. C 124 (25) (2020) 13706–13714.

[15] D. Chandler, Introduction to Modern Statistical Mechanics, Oxford Press, 1987.

[16] P. Hänggi, P. Talkner, M. Borkovec, Reaction-rate theory: fifty years after kramers, Rev. Modern Phys. 62 (1990) 251–341, http://dx.doi.org/10.1103/RevModPhys.62.251, URL https://link.aps.org/doi/10.1103/RevModPhys.62.251.

[17] H.O. Ron Elber, Dmitrii E. Makarov, Molecular Kinetics in Condensed Phases: Theory, Simulation, and Analysis, John Wiley & Sons, Newark, 2020.

[18] M.J. Weaver, Dynamical solvent effects on activated electron-transfer reactions: principles, pitfalls, and progress, Chem. Rev. 92 (3) (1992) 463–480.

[19] Z.-D. He, Y.-X. Chen, E. Santos, W. Schmickler, The pre-exponential factor in electrochemistry, Angew. Chem. Int. Ed. 57 (27) (2018) 7948–7956.

[20] I. Ledezma-Yanez, W.D.Z. Wallace, P. Sebastián-Pascual, V. Climent, J.M. Feliu, M.T.M. Koper, Interfacial water reorganization as a pH-dependent descriptor of the hydrogen evolution rate on platinum electrodes, Nature Energy 2 (4) (2017) 17031.

[21] J. Huang, P. Li, S. Chen, Quantitative understanding of the sluggish kinetics of hydrogen reactions in alkaline media based on a microscopic Hamiltonian model for the volmer step, J. Phys. Chem. C 123 (28) (2019) 17325–17334.

[22] P. Li, Y. Jiang, Y. Hu, Y. Men, Y. Liu, W. Cai, S. Chen, Hydrogen bond network connectivity in the electric double layer dominates the kinetic pH effect in hydrogen electrocatalysis on Pt, Nat. Catal. (2022) http://dx.doi.org/10.1038/s41929-022-00846-8, https://doi.org/10.1038/s41929-022-00846-8,

[23] F. Grün, M. Jardat, P. Turq, C. Amatore, Relaxation of the electrical double layer after an electron transfer approached by Brownian dynamics simulation, J. Chem. Phys. 120 (20) (2004) 9648–9655, http://dx.doi.org/10.1063/1.1718201, https://doi.org/10.1063/1.1718201.

[24] R. Kubo, Statistical-mechanical theory of irreversible processes. I. General theory and simple applications to magnetic and conduction problems, J. Phys. Soc. Japan 12 (6) (1957) 570–586, http://dx.doi.org/10.1143/JPSJ.12.570, https://doi.org/10.1143/JPSJ.12.570.

[25] R. Zwanzig, Time-correlation functions and transport coefficients in statistical mechanics, Annu. Rev. Phys. Chem. 16 (1) (1965) 67–102, http://dx.doi.org/10.1146/annurev.pc.16.100165.000435, https://doi.org/10.1146/annurev.pc.16.100165.000435.

[26] K.D. Fong, H.K. Bergstrom, B.D. McCloskey, K.K. Mandadapu, Transport phenomena in electrolyte solutions: Nonequilibrium thermodynamics and statistical mechanics, AIChE J. 66 (12) (2020) e17091, https://doi.org/10.1002/aic.17091, arXiv:https://aiche.onlinelibrary.wiley.com/doi/pdf/10.1002/aic.17091, URL https://aiche.onlinelibrary.wiley.com/doi/abs/10.1002/aic.17091.

[27] M.Z. Bazant, Theory of chemical kinetics and charge transfer based on nonequilibrium thermodynamics, Acc. Chem. Res. 46 (5) (2013) 1144–1160, pMID: 23520980 http://dx.doi.org/10.1021/ar300145c, https://doi.org/10.1021/ar300145c.

[28] Z. Zhang, Y. Gao, S. Chen, J. Huang, Understanding dynamics of electrochemical double layers via a modified concentrated solution theory, J. Electrochem. Soc. 167 (2019) 013519.

[29] R.F. Grote, J.T. Hynes, The stable states picture of chemical reactions. II. Rate constants for condensed and gas phase reaction models, J. Chem. Phys. 73 (6) (1980) 2715–2732, http://dx.doi.org/10.1063/1.440485, https://doi.org/10.1063/1.440485.

[30] O.K. Dudko, A. Szabo, Time-dependent rate coefficients for diffusion-influenced reactions with centrosymmetric potentials, J. Phys. Chem. B 109 (12) (2005) 5891–5894, pMID: 16851641 http://dx.doi.org/10.1021/jp044433q, https://doi.org/10.1021/jp044433q.

[31] I.V. Gopich, A. Szabo, Kinetics of reversible diffusion influenced reactions: The self-consistent relaxation time approximation, J. Chem. Phys. 117 (2) (2002) 507–517, http://dx.doi.org/10.1063/1.1482701, https://doi.org/10.1063/1.1482701.

[32] A. Molski, J. Keizer, Kinetics of nonstationary, diffusion-influenced reversible reactions in solution, J. Chem. Phys. 96 (2) (1992) 1391–1398, http://dx.doi.org/10.1063/1.462174, https://doi.org/10.1063/1.462174.

[33] A. Szabo, Theory of diffusion-influenced fluorescence quenching, J. Phys. Chem. 93 (19) (1989) 6929–6939, http://dx.doi.org/10.1021/j100356a011, https://doi.org/10.1021/j100356a011.

[34] B. Bagchi, Molecular Relaxation in Liquids, Oxford University Press, 2012.

[35] W. Schmickler, G. Belletti, P. Quaino, The approach of alkali ions towards an electrode surface – A molecular dynamics study, Chem. Phys. Lett. (ISSN: 0009-2614) 795 (2022) 139518, https://doi.org/10.1016/j.cplett.2022.139518, URL https://www.sciencedirect.com/science/article/pii/S0009261422001853.

[36] S.-J. Shin, H. Choi, S. Ringe, D.H. Won, H.-S. Oh, D.H. Kim, T. Lee, D.-H. Nam, H. Kim, C.H. Choi, A unifying mechanism for cation effect modulating C1 and C2 productions from CO2 electroreduction, Nature Commun. 13 (1) (2022) 5482, http://dx.doi.org/10.1038/s41467-022-33199-8, https://doi.org/10.1038/s41467-022-33199-8,

[37] T. Kumeda, L. Laverdure, K. Honkala, M.M. Melander, K. Sakaushi, Cations determine the mechanism and selectivity of alkaline ORR on Pt(111), 2022, http://dx.doi.org/10.48550/ARXIV.2205.00719, URL https://arxiv.org/abs/2205.00719.

[38] J. Resasco, L.D. Chen, E. Clark, C. Tsai, C. Hahn, T.F. Jaramillo, K. Chan, A.T. Bell, Promoter effects of alkali metal cations on the electrochemical reduction of carbon dioxide, J. Am. Chem. Soc. 139 (32) (2017) 11277–11287, pMID: 28738673 http://dx.doi.org/10.1021/jacs.7b06765, https://doi.org/10.1021/jacs.7b06765.

[39] J.D. Jackson, Classical Electrodynamics, John Wiley & Sons, 1975.

[40] J. Huang, M. Li, M.J. Eslamibidgoli, M. Eikerling, A. Groß, Cation overcrowding effect on the oxygen evolution reaction, JACS Au 1 (10) (2021) 1752–1765.

[41] X. Qin, H.A. Hansen, K. Honkala, M.M. Melander, Cation-induced changes in the inner- and outer-sphere mechanisms of electrocatalytic CO_2 reduction, 2022, preprint: https://doi.org/10.21203/rs.3.rs-2371405/v1.

[42] D.M. Heard, A.J.J. Lennox, Electrode materials in modern organic electrochemistry, Angew. Chem. Int. Ed. 59 (43) (2020) 18866–18884, https://doi.org/10.1002/anie.202005745, arXiv:https://onlinelibrary.wiley.com/doi/pdf/10.1002/anie.202005745, URL https://onlinelibrary.wiley.com/doi/abs/10.1002/anie.202005745.

[43] V. Palenskis, Drift mobility, diffusion coefficient of randomly moving charge carriers in metals and other materials with degenerated electron gas, World J. Condens. Matter Phys. 3 (1) (2013) 73–81.

[44] R. Memming, Semiconductor Electrochemistry, WILEY-VCH, 2001.

[45] J. Waelder, R. Vasquez, Y. Liu, S. Maldonado, A description of the faradaic current in cyclic voltammetry of adsorbed redox species on semiconductor electrodes, J. Am. Chem. Soc. 144 (14) (2022) 6410–6419, pMID: 35362961 http://dx.doi.org/10.1021/jacs.2c00782, https://doi.org/10.1021/jacs.2c00782.

[46] R. Vasquez, J. Waelder, Y. Liu, H. Bartels, S. Maldonado, A Gauss law analysis of redox active adsorbates on semiconductor electrodes: The charging and faradaic currents are not independent, Proc. Natl. Acad. Sci. 119 (36) (2022) e2202395119, http://dx.doi.org/10.1073/pnas.2202395119, arXiv:https://www.pnas.org/doi/pdf/10.1073/pnas.2202395119, URL https://www.pnas.org/doi/abs/10.1073/pnas.2202395119.

[47] H. Park, N. Kumar, M. Melander, T. Vegge, J.M. Garcia Lastra, D.J. Siegel, Adiabatic and nonadiabatic charge transport in Li–S batteries, Chem. Mater. 30 (3) (2018) 915–928, http://dx.doi.org/10.1021/acs.chemmater.7b04618, https://doi.org/10.1021/acs.chemmater.7b04618.

[48] N. Adelstein, J.B. Neaton, M. Asta, L.C. De Jonghe, Density functional theory based calculation of small-polaron mobility in hematite, Phys. Rev. B 89 (2014) 245115, http://dx.doi.org/10.1103/PhysRevB.89.245115, URL https://link.aps.org/doi/10.1103/PhysRevB.89.245115.

[49] C.S. Ahart, K.M. Rosso, J. Blumberger, Electron and hole mobilities in bulk hematite from spin-constrained density functional theory, J. Am. Chem. Soc. 144 (10) (2022) 4623–4632, pMID: 35239359, http://dx.doi.org/10.1021/jacs.1c13507, https://doi.org/10.1021/jacs.1c13507.

[50] J.M. Morbec, G. Galli, Charge transport properties of bulk Ta_3N_5 from first principles, Phys. Rev. B 93 (2016) 035201, http://dx.doi.org/10.1103/PhysRevB.93.035201, URL https://link.aps.org/doi/10.1103/PhysRevB.93.035201.

[51] B. Yan, D. Wan, X. Chi, C. Li, M.R. Motapothula, S. Hooda, P. Yang, Z. Huang, S. Zeng, A.G. Ramesh, S.J. Pennycook, A. Rusydi, Ariando, J. Martin, T. Venkatesan, Anatase TiO2—A model system for large polaron transport, ACS Appl. Mater. Interfaces 10 (44) (2018) 38201–38208, http://dx.doi.org/10.1021/acsami.8b11643, https://doi.org/10.1021/acsami.8b11643.

[52] J. Bisquert, The Physics of Solar Energy Conversion, CRC Press, 2022.

[53] F. Deißenbeck, S. Wippermann, Dielectric Properties of Nanoconfined Water from Ab Initio Thermopotentiostat Molecular Dynamics, J. Chem.Theory Comput. 19 (3) (2023) 1035–1043.

[54] A. Ojanperä, V. Havu, L. Lehtovaara, M. Puska, Nonadiabatic ehrenfest molecular dynamics within the projector augmented-wave method, J. Chem. Phys. 136 (14) (2012) 144103, http://dx.doi.org/10.1063/1.3700800, https://doi.org/10.1063/1.3700800.

[55] G. Kodis, M.Z. Ertem, M.D. Newton, D.V. Matyushov, Reorganization energy of electron transfer in ionic liquids, J. Phys. Chem. Lett. 13 (14) (2022) 3297–3303.

[56] E. Santos, W. Schmickler, Models of electron transfer at different electrode materials, Chem. Rev. 122 (12) (2022) 10581–10598.